

27-day variations in F_2 layer critical frequencies at Huancayo

JULIUS BARTELS

Geophysikalisches Institut University, Göttingen

(Received 14 February 1950)

ABSTRACT

The solar radiation responsible for the production of F_2 layer ionization is already known to change with the 11-year sunspot cycle. The question has therefore been examined whether analogous changes occur in the course of the solar rotation of about 27 days period in cases where the sunspot numbers R show appreciable quasi-persistent periodicities. After correcting for lunar tidal influence, variations of the type in question have been found in the noon values of fF_2 for Huancayo, Peru, using the superposed epoch method. Such variations are found to be of the order of 6 to 10%. Changes in fF_2 accompanying changes in R appear to be delayed by about two days, but a scatter analysis by means of synchronized harmonic dials throws doubt on the statistical significance of such a lag. The lunar tides in the noon values of fF_2 , examined for comparison, cause total semimensual changes of more than 10% in southern summer, but only 2 to 3% in southern winter. These seasonal changes in the lunar tidal effect $L(fF_2)$ are much larger than those disclosed in the quantitative effects of changes of R on fF_2 . The use of these results in ionospheric forecasting is briefly discussed.

THE PREPARATION OF THE OBSERVATIONAL DATA

The terrestrial effects of solar phenomena are often studied by considering changes of annual or monthly averages of solar and terrestrial quantities during the course of the 11-year sunspot cycle. Such results may be supplemented by the examination of cases where sunspots are unsymmetrically distributed in heliographic longitude and where the sun, in the course of a rotation in about 27 days, exhibits, alternatively, discs with many spots and with few spots. Such 27-day variations of solar activity (R) have, by the application of the superposed-epoch method, been shown to be accompanied by similar variations in the intensity of a solar influence W (wave-radiation) as inferred from the ranges of the solar-diurnal variation, Sq , in the horizontal magnetic intensity H at Huancayo, Peru (BARTELS [2]). Analogous results are described here for the noon values of the ionospheric critical frequency fF_2 observed at Huancayo.

The procedure followed resembles that described in the earlier paper cited. It involves the following steps:

(a) From the published hourly fF_2 values for January 1938 to June 1946 (WELLS and BERKNER [11]) daily averages of the 5 hourly values 1000 to 1400 h (Eastern Standard Time, 75th meridian) are computed and referred to as noon values.

(b) The semi-mensual waves due to the lunar ionospheric tide $L(fF_2)$ are eliminated using results of an analysis already made [3].

(c) Days which were magnetically disturbed by solar particle radiation (P) before 1400 h, as indicated by the K -indices (IATME [8]), are omitted; these are

mainly days with international magnetic character figure $C = 1.7$ or higher. In addition, the immediately succeeding days were omitted in order to be free from the after-effects of such disturbances. Other gaps in the data occur where no records are available because of reflection or of absorption by lower layers or for other reasons.

(d) The material is divided into conventional solar rotation intervals of exactly 27 days; for example, the first day of rotation No. 1501 is Dec. 28th, 1942. These were further divided into intervals of 27/8 days, called eighths of rotations and designated $a, b, \dots h$.

(e) Averages of the daily noon values of fF_2 , corrected for $L(fF_2)$ are computed for eighths of rotations (eighth-values); for that purpose, gaps in the series are bridged by interpolations.

Figs. 1 and 2—Typical plots of consecutive daily values of sunspot-numbers R and of noon-values of critical frequency fF_2 , (corrected for the lunar influence) for southern summer (December and January) and southern winter (June and July), for intervals near sunspot-maximum (1938/39) and near sunspot-minimum (1943/44).

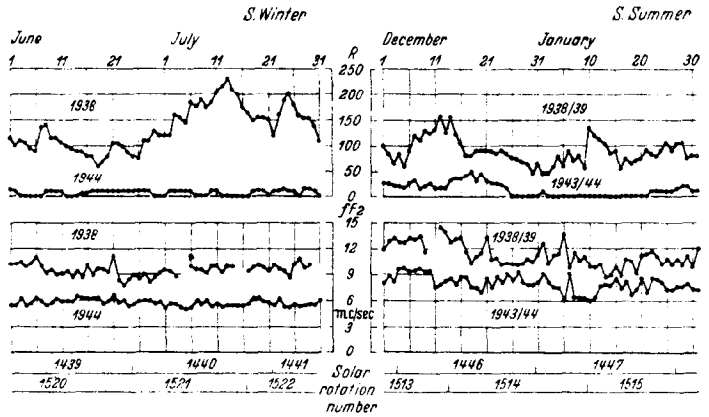


Fig. 1.

Fig. 2.

(f) From the eighth-values running averages for 27-day intervals are derived.

(g) These averages are subtracted from each eighth-value to compute "eighth-deviations" Δf .

(h) Averages are formed of Δf to obtain "three-eighth deviations" $\Delta 3f$; these are practically equivalent to the deviations of 10-day means from 27-day means.

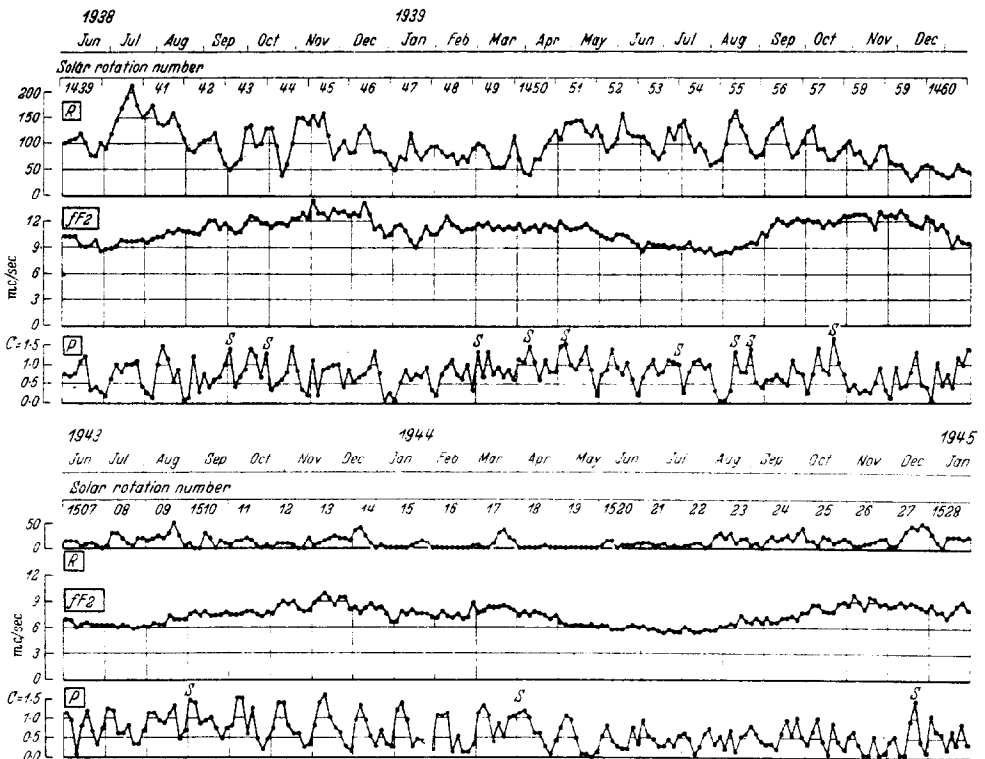
For comparison, eighth-values, eighth-deviations and three-eighth-deviations are available for Zürich relative sunspot-numbers R (a unit of R will be denoted by z), for solar wave-radiation W as derived from $Sq(H)$ at Huancaayo, and for solar particle-radiation P based on C values. The tables for these data [2] have been continued for R and P up to 1949; W -values end with the end of the published magnetic readings, 1944.

The changes in the course of the 11-year cycle are so great that the values for 1938/39 (near sunspot-maximum) and for 1943/44 (near minimum) could be plotted in the same graph (Figures 1 and 2). The seasonal variation in fF_2 is clearly seen (higher values in summer). But it is difficult to recognize, by mere inspection,

clear relations between the day to day changes in R and fF_2 in Figures 1 and 2. This is partly due to the uncertainty in the physical definition of the daily values of R , which, as has been already pointed out (BARTELS [2], p. 232), is reflected in the day to day variations of sunspot-numbers assigned either by Zürich (R_Z) or American observatories (R_A). For an example of such differences the following may be quoted [7], [10]:

1949 June (Day)	11	12	13	14	15	16
$R_Z =$	102	86	119	114	85	103
$R_A =$	104	120	143	97	102	123

It is for this reason that this investigation is based on eighth values and eighth deviations.



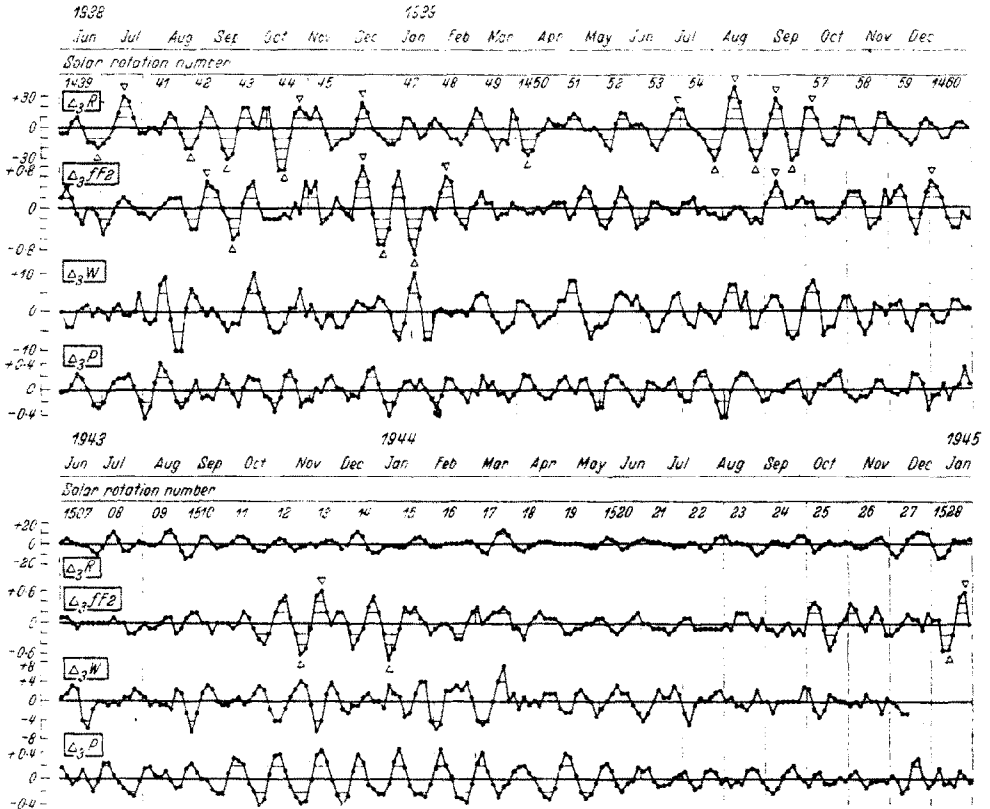
Figs. 3 and 4—Eighth-values (that is, eight values per solar rotation of 27 days) for sunspot-numbers R , noon-values of critical frequency fF_2 at Huancayo, and solar particle-radiation P , for two intervals of 22 rotations each, near sunspot-maximum and near minimum.

The eighth-values shown in Figures 3 and 4 include intervals for which daily values were shown in Figures 1 and 2. The smooth run of the fF_2 -eighths, especially in southern winter, is noteworthy. In P , eighths containing days with storms ($C = 1.9$ or 2.0) are marked by an S . Since such days, along with those with $C = 1.7$ or 1.8 , were omitted in computing the fF_2 -eighths, the apparent independence of fF_2 from P shown in the diagrams refers only to changes of P between

$C = 0.0$ and 1.6 . Similarly it is not easy to infer, from a comparison of the curves for R and fF_2 , those definite relationships for variations within one rotation found in the following analysis.

SYNCHRONIZATION EXPERIMENTS

The general idea of these statistical experiments has been described in an earlier paper [2]. The epochs to be superposed were selected as maxima or minima according to $\Delta 3R$ in Experiments Nr. 1 and 3, and according to $\Delta 3f$ in the twin



Figs. 5 and 6—Three-eighths-deviations ($=10$ -days-means minus 27 -days-means) for the same intervals as in Figures 3 and 4; relative to the scales in Figures 3 and 4, the ordinates are magnified 2-fold in R , 6-fold in fF_2 , and $(5/3)$ fold in P .

Exps. Nr. 2 and 4. The rule adopted in selecting pulses in R was that the sum of three consecutive values of $\Delta 3R$ should deviate from zero by $50z$ ($= 50$ Zürich units) or more. This gave $n = 24$ positive pulses for Exp. 1, and 21 negative pulses for Exp. 3. For the twin experiments (selection in $\Delta 3f$), nearly equal numbers n of epochs were obtained by adopting the rule that the sum of three consecutive values of $\Delta 3f$ should deviate from zero by 1.1 mc/sec (1 mc/sec $= 10^6$ cycles per second) or more; this gave $n = 23$ positive pulses (Exp. 2) and 24 negative pulses (Exp. 4). The selected epochs shown in Figures 5 and 6 are indicated by triangular marks above the positive pulses and below the negative pulses. Figure 7 gives a complete list.

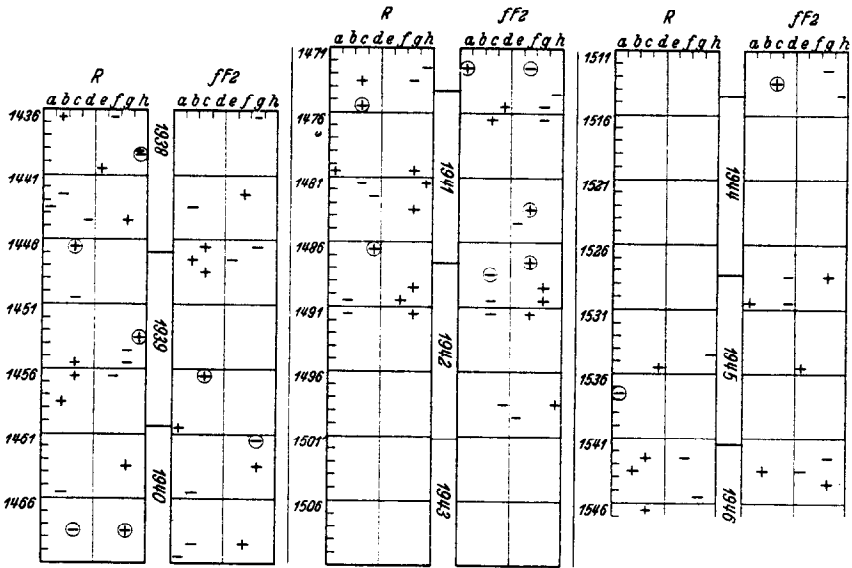


Fig. 7—Selected epochs in R and fF_2 in the solar rotation intervals 1436 to 1546. Encircled symbols mark those epochs which were omitted at a later stage (harmonic analysis).

Some selected epochs of the same sign in R and fF_2 occur less than 2 eighths apart. A few such "coincident pulses" are shown in Figure 5 as 1443 a/b, 1446 c, 1456 c. In all, 10 positive pulses and 7 negative pulses were found to be coincident in the sense defined above, that is, about 3 to 4 pulses out of every 10 selected pulses; this indicates already a high degree of correlation between R and fF_2 .

The procedure of synchronization starts with copying, for each selected epoch (e.g., eighth 1436 b, a positive pulse in R), a row with the eighth-deviations ΔR

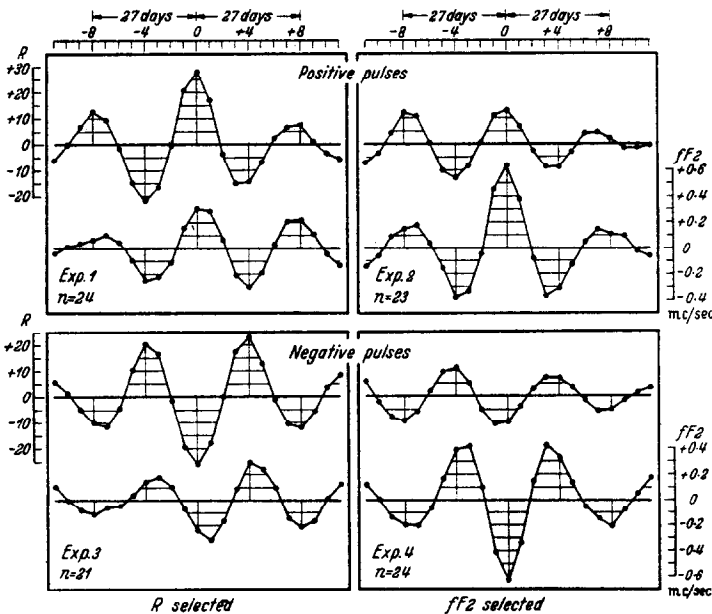


Fig. 8—Results of synchronization experiments for sunspot numbers R and critical frequencies fF_2 at Huancaayo. n =number of epochs superposed.

for 25 consecutive eights, with the selected epoch in the centre, and another row with the simultaneous values ΔfF_2 . The whole material for Exp. 1, for example, consists of two matrices, one for ΔR and one for ΔfF_2 . Each matrix has $n = 24$ rows, one for each selected epoch, numbered $k = 1, 2, \dots, 24$, and 25 columns numbered eighth $- 12, - 11, \dots, - 1, 0$ (= selected epoch), $+ 1, + 2, \dots, + 12$. The arithmetic averages of the 25 columns give the "average row"; it is smoothed by overlapping means, as $(a + b + c)/3$, to obtain the average three-eighths deviations shown in Figure 8. This figure giving the main result of this paper, should be compared with the analogous diagram in the earlier paper [2].

Figure 8 suggests that the average selected pulse in one of the phenomena compared, R or fF_2 , is accompanied by an average pulse of the same sign in the other phenomenon. The following scatter analysis determines the quantitative relations, and decides whether the slight lag of the pulses in fF_2 is statistically significant.

HARMONIC ANALYSIS

In this study every rotation centred at a selected epoch is considered, *e.g.*, the 9 values for the eighths $- 4$ to $+ 4$. A time variable t_k is chosen, with $t_k = 0^\circ$ at the k 'th selected epoch, and increasing from $- 180^\circ$ to $+ 180^\circ$ during the rotation considered. Harmonic analysis yields $s_k \cos(t_k - \sigma_k)$ for the selected pulse and $c_k \cos(t_k - \gamma_k)$ for the co-ordinated pulse. It is convenient to apply the signs (plus and minus) of the selected pulses to the amplitudes s_k as well as c_k , so that phase angles σ_k near zero will prevail for the selected pulses.

The usual harmonic dial representation (CHAPMAN and BARTELS [6], p. 563) for Exp. 1, with positive pulses selected in R (Figure 9), shows, in the dial for R (left), the 24 individual selected pulses by as many dots as end points of vectors determined by their lengths s_k from the origin, and their angular deviations σ_k from the vertical towards the right. Similarly, the dial for the co-ordinated pulses in fF_2 shows the vectors $(c_k \gamma_k)$. The angular scale of each dial expresses σ_k and γ_k as the delay, in days, of the maximum of the cosine wave after the zero epoch. The 5 selected positive pulses in R with the smallest s_k (equal to 20 z or less) are indicated by smaller dots; they were omitted from the further discussion, which is thereby restricted to 19 pulses only. The mass centres of the 19 dots, represent the average relation between the 19 pulses; they appear in Figure 9 as the end points of the two heavy lines (average vectors) drawn from the origins of the two dials. Numerically, the average selected pulse in R is $34 z \cos(t + 4^\circ)$ and the average co-ordinated pulse in fF_2 is $0.35 \cos(t - 16^\circ)$ mc/sec. This means that the ratio of the amplitudes is $r = 97 z / \text{mc/sec}$, and that the average maximum in fF_2 is delayed, against R , by $4^\circ + 16^\circ = 20^\circ$, or $20^\circ \cdot 27 d / 360^\circ = 1.5 d$.

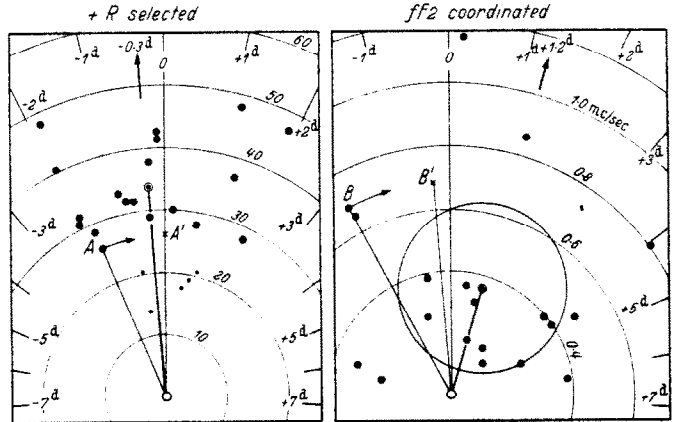
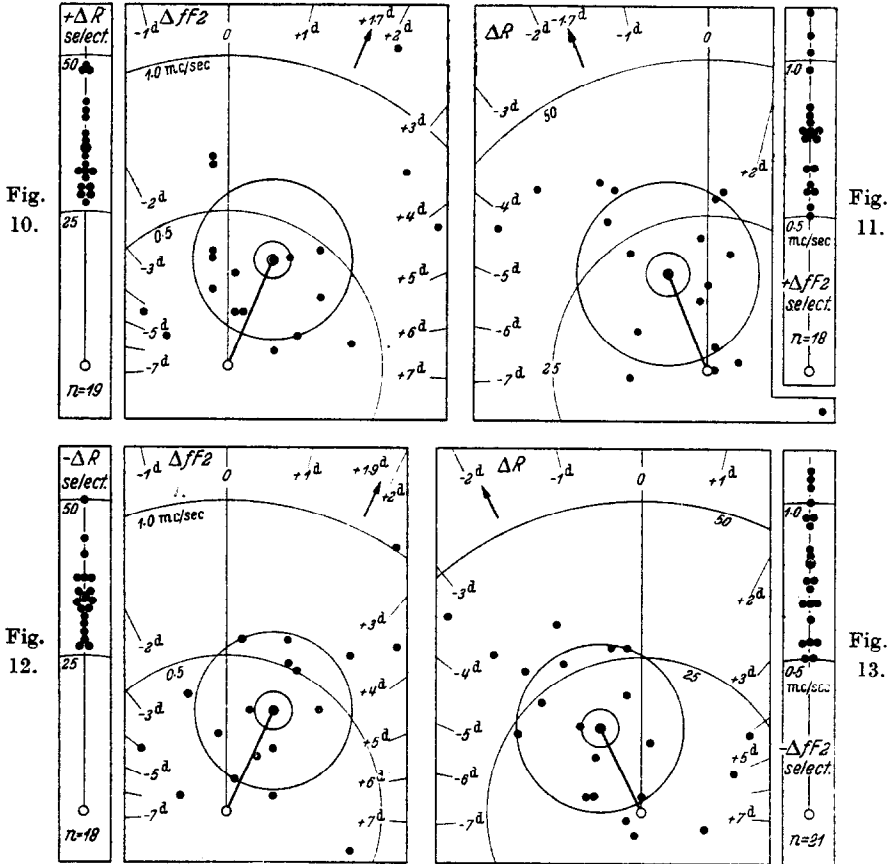


Fig. 9—Harmonic dials for Experiment No. 1.

Figure 9), shows, in the dial for R (left), the 24 individual selected pulses by as many dots as end points of vectors determined by their lengths s_k from the origin, and their angular deviations σ_k from the vertical towards the right. Similarly, the dial for the co-ordinated pulses in fF_2 shows the vectors $(c_k \gamma_k)$. The angular scale of each dial expresses σ_k and γ_k as the delay, in days, of the maximum of the cosine wave after the zero epoch. The 5 selected positive pulses in R with the smallest s_k (equal to 20 z or less) are indicated by smaller dots; they were omitted from the further discussion, which is thereby restricted to 19 pulses only. The mass centres of the 19 dots, represent the average relation between the 19 pulses; they appear in Figure 9 as the end points of the two heavy lines (average vectors) drawn from the origins of the two dials. Numerically, the average selected pulse in R is $34 z \cos(t + 4^\circ)$ and the average co-ordinated pulse in fF_2 is $0.35 \cos(t - 16^\circ)$ mc/sec. This means that the ratio of the amplitudes is $r = 97 z / \text{mc/sec}$, and that the average maximum in fF_2 is delayed, against R , by $4^\circ + 16^\circ = 20^\circ$, or $20^\circ \cdot 27 d / 360^\circ = 1.5 d$.

IMPROVED SYNCHRONIZATION

The above method can be improved as follows. From the selection of the epochs it follows that the maxima of the selected cosine waves will not deviate much from zero epoch. There remains, however, a scatter of those maxima (Figure 9, left) between $-2d$ and $+2d$ which hampers the comparison with the point cloud



Figs. 10 to 13—Harmonic dials for the improved synchronizations showing individual selected and co-ordinated pulses, corresponding to Exps. No. 1 to 4 in Figure 8.

in the dial of co-ordinated pulses (Figure 9, right). Consider, for instance, the pulse 1491 *g*, represented by the dots marked *A* and *B* in the two dials. The improvement consists in turning the "selected" vector *OA* into the vertical (position *OA'*), and the "co-ordinated" vector *OB* by the same angle *AOA'* into the position *OB'*. With such a phase angle correction applied to all pulses the vectors for the selected pulses will all become vertical, and the scatter of phases in the "synchronized" dial for the co-ordinated pulses will indicate the degree of correlation between the two phenomena. For this correction the phase angles of selected pulses with small amplitudes s_k are not sufficiently significant; this is the reason why those pulses were omitted, and with them their co-ordinated pulses. This improvement of Figure 9 is shown as Figure 10; similarly, Figures 11 to 13 show the individual pulses used in the Exps. 2 to 4 of Figure 8.

It is easy to suggest more detailed methods for studying the transformation of the point cloud of selected pulses into that for the co-ordinated pulses—for instance, to reduce all selected vectors to the same amplitude—but the number of dots in each dial is too small for an application. A summarizing measure for the amount of scattering of the co-ordinated pulses is indicated by the “probable error circle” (large circle around the mass centre) constructed so as to contain $n/2$ of the n individual dots; the smaller circle with a radius smaller in the ratio $n^{-1/2}$ is the probable error circle for the average vector. It is realized, of course, that this is a rough statistical treatment, because the distribution in the dial of selected pulses is linear, and the transformation of that point cloud into the dial of co-ordinated pulses will not lead to a circular distribution. Furthermore, the “effective number of independent cases” will certainly be smaller than n , because many of the pulses occur in the same or consecutive rotations (see Figure 7) and will therefore not be independent.

As the main result of this paper, the evidence for the positive correlation between pulses in R and fF_2 seems conclusive. The time lag of fF_2 behind R is suggestive but not quite beyond doubt; the satisfactory agreement of the four experiments in that respect appears to be less significant if the non-independence of the pulses is remembered.

QUANTITATIVE RELATIONS BETWEEN AVERAGE PULSES

Figures 1 to 6 have shown that the magnitude of the variations of fF_2 are smaller in southern winter. This is also borne out by the fact that, of the $23 + 24 = 47$ pulses selected in fF_2 , not more than 2 pulses fall in the 4 winter months centred at the June solstice. Hence, the following attempt to arrive at a quantitative comparison of the harmonic amplitudes s and c of the average selected and co-ordinated pulses is restricted, in R also, to the pulses in the other 8 months (non-winter). Furthermore those pulses with small s_x which had been omitted in the dials are excluded. The following rows give the number n of pulses considered, and—judged from the mass centres of the dots in the dial—average amplitudes for R in Zürich units z , and for fF_2 in mc/sec , as well as the phase-lag of fF_2 behind R ;

- + pulses in R . $n = 12$: $s = 35.2 z$, $c = 0.44 mc/sec$, lag 1.1 d .
- pulses in R . $n = 12$: $s = 36.2 z$, $c = 0.40 mc/sec$, lag 1.6 d .
- + pulses in fF_2 . $n = 18$: $c = 16.7 z$, $s = 0.77 mc/sec$, lag 1.7 d .
- pulses in fF_2 . $n = 21$: $c = 15.2 z$, $s = 0.77 mc/sec$, lag 2.0 d .

The combined positive and negative pulses, selected in R , give the ratio of the amplitudes $r = 35.7/0.42 = 85 z/mc/sec$, while those selected in fF_2 give $r = 16.0/0.77 = 21 z/mc/sec$. The difference between these two ratios is the effect of statistical regression (BARTELS [2]). As a single value for r —uncertain as it may be—the ratio of the averages of the four amplitudes may be adopted, which leads to a change of $r = 43$ Zürich units in R for a change of 1 mc/sec in the noon values of fF_2 ; this refers to the 8 months September to April at Huancayo.

This effect of R on fF_2 for changes occurring in 27 days rotations should be compared with the analogous effect in the course of the 11 years' cycle. Average diurnal variations of the monthly median values of fF_2 (WELLS and BERKNER [11]), computed separately for months with high and low sunspot numbers, yield, for the noon values, ratios r between 21 and 22 $z/mc/sec$ for the 8 months con-

sidered above, and $r = 32$ for the 4 winter months May to August. The nomogram (PHILLIPS [9], p. 328) for the corresponding annual means of the noon values for fF_2 and of R gives $r = 25$, which confirms the ratios given above. All have the same order of magnitude as the ratio $r = 21$ derived above from 27-days pulses selected in fF_2 which, for statistical reasons, is likely to be an underestimate for r , unless it is assumed that the changes in ΔfF_2 depend on nothing else but the changes in ΔR .

The sensitivity of fF_2 with regard to changes in R seems, therefore, to be somewhat higher for changes in the course of the 11 years' cycle than in the course of a solar rotation, but not more than twice as large. This result should not be stressed too much, however, for reasons given in a previous discussion of the similar problem regarding W (BARTELS [2], pp. 224ff. and 238ff.). The smaller number of observations available for fF_2 prohibits a repetition of the more detailed treatment applied in the case of W , such as the standardization (l.c. p. 185) aimed at the elimination of the seasonal effects.

The seasonal change in the relation of fF_2 to R can be studied in the pulses selected for R , separated for winter (months May to August) and non-winter (the other 8 months). In order to increase the number of pulses in each sub-division the negative pulses were inverted and combined with the positive pulses.

Winter: $n = 13$; $s = 35.1 z$, $c = 0.28$ mc/sec, lag 3.0 *d*.

Non-winter: $n = 24$; $s = 35.7 z$, $c = 0.42$ mc/sec, lag 1.4 *d*.

The effect of R on fF_2 in winter appears to be about 2/3 of what it is in non-winter. The absolute noon values of fF_2 , judged from the average 27-days means centred at the selected epochs considered, increase, from winter to non-winter, from 8.3 to 10.7 mc/sec. A relative change in fF_2 by 5%, or in the equivalent electron concentration N by about 10%, is therefore caused by changes in R by 49z in winter, and 46 z, practically the same amount, in non-winter. In order to correct for the influence of regression the figures should be reduced to about a half, or 24 z. In the 11 years' cycle, relative changes of the noon values of fF_2 by 5% were found to correspond to changes in R by 12.8z in winter, 10.4z in non-winter. The seasonal decline in winter of the response of fF_2 to changes in R is somewhat larger in that material than in the 27-days variations discussed above.

For non-winter, the cases can be further divided into coincident and non-coincident pulses; again, averages of positive pulses and inverted negative pulses are given:

Coincident pulses,
 selected in R , $n = 14$: $s = 35.8 z$, $c = 0.56$ mc/sec, lag 1.7 *d*,
 selected in fF_2 , $n = 12$: $c = 29.1 z$, $s = 0.83$ mc/sec, lag 2.7 *d*,
 Non-coincident pulses,
 selected in R , $n = 10$: $s = 36.1 z$, $c = 0.24$ mc/sec, lag 0.2 *d*,
 selected in fF_2 , $n = 25$: $c = 8.5 z$, $s = 0.76$ mc/sec, lag 1.0 *d*.

The difference in the ratios s/c and c/s for the twin experiments is, of course, strongest for the non-coincident pulses; the time lags, however, even for those pulses, agree satisfactorily.

The synchronizations suggest 1.6 days as the best value for the time lag of the extremes of the daily values of ΔfF_2 after those of ΔR . A correction is necessary because the times of the observations differ (BARTELS [2], p. 224; the corrected values for the lag of W given below have been derived from increased material).

The daily Zürich values for R refer, roughly, to about 07 GMT, while those for fF_2 refer to Huancayo noon, 17 GMT, which is 10 hrs = 0.4 d later. The corrected time lag of fF_2 is, therefore, 2.0 days; the standard error will not exceed one day. This may be compared with the time lag of 1.8 days, after R , found for the geomagnetic W -measure of solar ultraviolet radiation, for 111 pulses (63 positive, 48 negative) selected in R in the years 1922–1944. The lags in fF_2 and W appear practically identical. It must be mentioned, however, that for those pulses in R , in the years 1938 to 1944, for which simultaneous observations of fF_2 and W are available, the individual co-ordinated pulses in fF_2 and W show little correlation with each other, beyond the general occurrence of average pulses in fF_2 and W accompanying those in R .

There is an apparent asymmetry in the two secondary pulses, occurring one rotation before and after the main pulse as a result of the 27-days recurrence tendency (Figure 8). The symmetry shown by the secondary pulses which accompany the selected pulse is not repeated in those which accompany the co-ordinated pulses. For instance, in Exp. 1, in fF_2 , the following secondary pulse is stronger than the preceding secondary pulse. A similar increase of the ratio of the pulse strengths in fF_2 relative to those of the simultaneous secondary pulses in R is also shown in Exps. 2 to 4. This might indicate that the influence of solar spot-regions on fF_2 increases with their lifetimes, and might be related to the lags found by ALLEN [1] in correlations of monthly means.

COMPARISON OF SOLAR AND LUNAR INFLUENCES

In southern summer, the total systematic change of the noon values of fF_2 with the moon's phase is as great as 1.1 mc/sec; in January and February, for example, this is the amount by which the noon values about an eighth of a synodic month before New or Full Moon exceed those about an eighth of a month after those dates (BARTELS [3]). The semi-mensual (CHAPMAN [5]) tidal effect of the moon on the daily noon values of fF_2 is, therefore, greater than the effects of R shown in Figure 8. This is also demonstrated by Figure 14, which shows as ordinates all the noon values used in this paper, expressed as deviations from 27-days averages, and distributed according to the mean moon's phase (abscissae), numbers μ decreasing from 24 to 0 from New Moon to New Moon (448 days in January and February, 454 days in June and July).

In June and July (southern winter) the total change due to the lunar tidal influence is reduced to 0.2 mc/sec. The reaction of fF_2 to lunar tidal influences, of semi-mensual period, is thus shown to have a stronger seasonal variation than its reaction to solar influences, of solar rotation period.

As Figure 14 shows, the scatter of the individual daily noon values of fF_2 varies, with season, just as the amplitude of $L(fF_2)$. This supports the hypothesis that the irregular changes of fF_2 from day to day are, largely, to be considered as changes in the intensity of $L(fF_2)$; similar indications have been found in the geomagnetic tides $L(H)$ at Huancayo [4].

For the separation of solar and lunar effects, it is fortunate that the periods 14.77 d for half a synodic month and about 27 d for the solar rotation do not interfere. It is difficult to separate the full period of the month, 29.53 d , from the quasi-persistent periodicities connected with the solar rotation. Because of the superposed solar effect, the noon values (Figure 14) are less suitable for the studies of the variability of $L(fF_2)$ than, for instance, the daily changes of fF_2 from 11 to 18 h local time [3].

JULIUS BARTELS: 27-day variations in F_2 layer critical frequencies at Huancayo

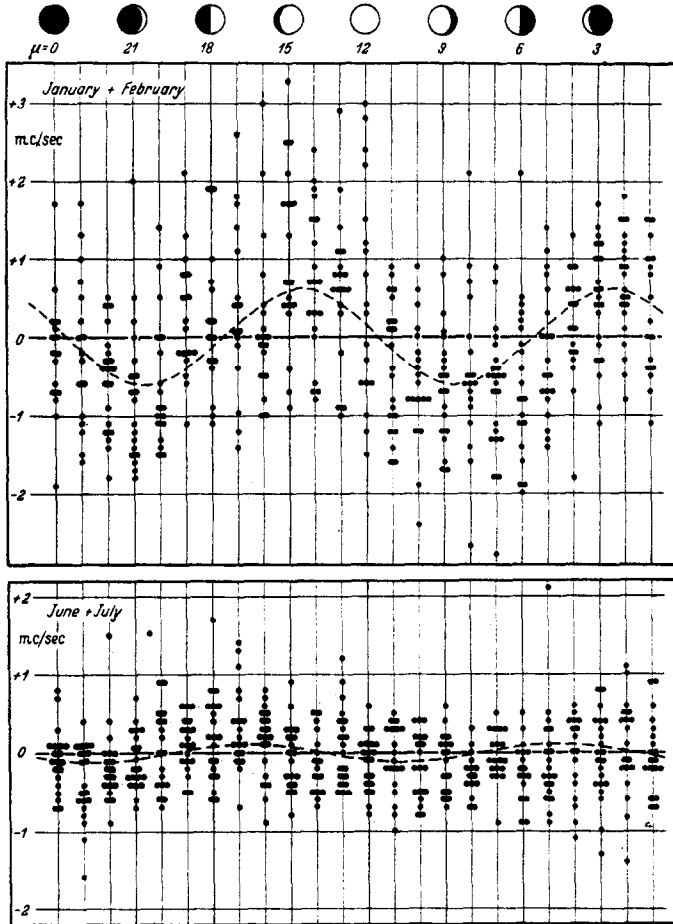


Fig. 14—Daily noon-values of fF_2 at Huancayo, on undisturbed days, in deviations from 27-days averages, arranged according to the phase μ of the mean moon, to show lunar tidal influence in the course of a lunar month.

USE IN PRACTICAL PREDICTION

The usual prediction of fF_2 for use in radio propagation is restricted to monthly averages. The results described here indicate that the predictions might occasionally be refined by taking into account the quasi-persistent periodicities due to long lived active centres confined to one half of the Sun. If this should be found practicable the lunar influence, which is often larger than that solar effect, should also be taken into account.

REFERENCES

[1] ALLEN, C. W.; Terr. Magn. 1946 51 1; Terr. Magn. 1948 53 433. [2] BARTELS, J.; Terr. Magn. 1946 51 181. [3] BARTELS, J.; $L(fF_2)$ at Huancayo, Prelim. note in Ber. dtsh. Wetterdienst US-Zone (Bad Kissingen) 1949 12 30. [4] BARTELS, J. and JOHNSTON, H. F.; Terr. Magn. 1940 45 269, 485. [5] CHAPMAN, S.; Terr. Magn. 1942 47 279. [6] CHAPMAN, S. and BARTELS, J.; Geomagnetism. Oxford: Univ. Press 1940. [7] CRPL 1949. Central Radio Propag. Lab. F 59, Ionospheric Data, issued July 1949. Washington, Nat. Bur. of Standards. [8] IATME (Int. Assoc. Terr. Magn. Electr., in the Int. Union of Geodesy and Geophys.), Bull. 12 (1947), 12A (1948), 12B (1949). [9] PHILLIPS, M. LINDEMAN; Terr. Magn. 1947 52 321. [10] WALDMEIER, M.; Final sunspot-numbers for 1949 (in press 1950). [11] WELLS, H. W. and BERKNER, L. V.; 1947 Carnegie Inst. Washington Publ. 175 (Res. Dept. Terr. Magn.) Vol. XI.